Electromagnetic Geophysics Techniques for Location of Abandoned Underground Mines

Dr. Ben K. Sternberg
Professor, and Director, Laboratory for Advanced Subsurface Imaging
University of Arizona
Tucson, Arizona 85721-0012
bkslasi@u.arizona.edu

Abstract

The Laboratory for Advanced Subsurface Imaging (LASI) at the University of Arizona has been involved in the development of electromagnetic geophysics techniques for location of abandoned underground mines and other subsurface voids and tunnels since 1992. One of the systems that we developed is known as the LASI ellipticity system. This electromagnetic sounding system uses transmitter and receiver coils mounted on All Terrain Vehicles (ATVs). The frequency is swept from 1 kHz to 1 MHz or 30 kHz to 30 MHz. Measurements of the ellipticity of the magnetic field are converted to electrical resistivity versus depth at each measurement location. A cross section of the earth is displayed as the electromagnetic fields are recorded along a profile line.

The LASI ellipticity system was used to survey an area over the abandoned Union Pacific #9 coal mine near Rock Springs, Wyoming. A portion of the mine is subsiding due to a fire in the coal seam. The locations of subsidence-prone zones were successfully mapped by the system. We also mapped a tunnel located at our Avra Valley Geophysical Test Site and an access tunnel at the Nevada Test Site.

We have used ground penetrating radar (GPR) with a center frequency of 16 MHz to map underground mines at Tombstone, Arizona. GPR surveys along Allen and Toughnut streets showed the locations of the abandoned underground workings and the subsidence prone regions. We have also conducted other GPR surveys in southern Arizona, which have successfully mapped tunnels.

Our most recent research involves the development of a new electromagnetic imaging system in the frequency range from 1 to 100 MHz. Because of new FCC restrictions, it is now virtually impossible to transmit wideband GPR signals at frequencies less than 100 MHz. Unfortunately, frequencies below 100 MHz are required for mapping features related to abandoned underground mines. Our approach is to use the available Industrial, Scientific and Medical (ISM) frequencies at 6.78, 13.56, 27.12, and 40.68 MHz. We then use a method known as Model Based Parameter Estimation (MBPE) to predict the earth response at other frequencies. We are currently in the development and testing phase for this method.

Introduction

The Laboratory for Advanced Subsurface Imaging (LASI) at the University of Arizona has been involved in the development of electromagnetic geophysics techniques for location of abandoned underground mines and other subsurface voids and tunnels since 1992. I will review some of the technology that we have used, as well as discuss a series of case histories, which illustrate the capabilities of these methods.

The LASI ellipticity system

With Department of Energy funding, we developed an electromagnetic imaging system in the frequency range from 30 kHz to 30 MHz. The primary applications for this system were in imaging the location of buried waste and contaminated ground water. With Department of Defense and Bureau of Mines funding, we developed an electromagnetic imaging system in the frequency range from 1 kHz to 1 MHz. The primary applications for this system were in imaging the location of abandoned mine workings and subsurface voids. The details of the ellipticity system have been published in Sternberg (1999), Sternberg et al. (1999), and Sternberg and Birken (1999).

In these systems, a transmitter generates a swept-frequency signal in one of the two frequency ranges. We record the ellipticity of the magnetic field at a receiver. The received magnetic field over the earth traces out an ellipse as a function of time. The ellipticity is defined as the ratio of the minor axis to the major axis of this ellipse. The ellitpticity provides diagnostic responses over earth structures of interest. Figure 1 shows the transmitter system mounted on an all terrain vehicle (ATV). Figure 2 shows the receiver system mounted on a second ATV. During operation, these two ATVs move along a profile line, recording the ellitpticity versus frequency. We then invert these data to cross sections of resistivity versus depth using various modeling programs. The depth of investigation varies with the resistivity conditions and will be shown for specific targets in the following case histories.

Tunnel at the Avra Valley Geophysical Test Site

We have developed a test site west of the University of Arizona campus known as the Avra Valley Geophysical Test Site (Sternberg et al., 1991). It is located approximately 3.8 km west of Ryan field on Ajo Way. The site contains a wide variety of buried targets, including various metal containers simulating buried waste and water injection basins. The site has been used by many groups to test geophysical techniques and can be made available to other interested researchers.

Figure 3 shows a buried concrete pipe or tunnel, approximately 1 m diameter, and buried 3m to the center of the pipe. Figure 4 shows the recorded 8 kHz ellipticity data over this pipe/tunnel (from Sternberg and Poulton, 1995). There is a strong response over this concrete pipe, i.e. much larger than the background variations in the soil.

Tunnel at the Nevada Test Site

The next test was over a deeper tunnel, located at the Department of Energy's planned waste site at the Nevada Test Site. The tunnel is approximately 30 m deep. It is currently being used as an access tunnel for tests on the suitability of the site for storage of high-level nuclear waste. The tunnel contains many metal pipes. We used a sheet modeling program to model the data (Sternberg and Yang, 1999). Figure 5 shows the model that was used for the theoretical electromagnetic response calculations. Figure 6 shows the measured 4 kHz ellipticity data over the tunnel and the sheet model calculations (Sternberg and Poulton, 1996). There are significant variations in the measured data due to the normal variations in rock resistivity but there is still a distinct anomaly visible that is due to the tunnel. The calculated model data agree well with the measured data.

Subsidence region over a burning coal mine

The next case history was from a survey sponsored by the U.S. Bureau of Mines (Poulton and Sternberg, 1995). The survey was over the abandoned Union Pacific #9 coal mine near Rock Springs, Wyoming (Figure 7). A portion of the mine is subsiding due to a fire in the coal seam. Figure 8 shows the results of one of our ellipticity survey lines. In this case, the ellipticity data were converted to a resistivity versus depth cross section. A locally one-dimensional modeling code was applied at each measurement location. The resulting resistivities versus depth were then contoured to produce this map. The green color on the left in this plot shows the normal background resisitivity for the rocks in this area. The dark blue color on the right shows anomalously low resistivities. These low resisitivities are interpreted to be due to water-containing fractures caused by the subsidence zone above the burning coal mine. This region correlates well with the known extent of the currently burned coal mine area.

Ground penetrating radar survey at Tombstone, Arizona

We have also used commercial ground penetrating radar (GPR) equipment for locating abandoned underground mine workings. We used a Geophysical Survey Systems (GSSI) SIR-8 GPR with a model 3200, 16 MHz antenna, and GRORADAR data acquisition and processing software. This GPR operates in the time domain and transmits a short pulse into the ground. Any reflections resulting from contrasts in the electrical properties in the subsurface are recorded versus time. Figure 9 shows the location of the survey in Tombstone, Arizona. Figure 10 shows the results of the GPR survey at Toughnut Street (Henley and Sternberg, 2000). The warmest colors show the areas of highest reflection signal strength. The cool colors show the normal background signal strength. The time scale has been converted to depth based on velocities determined from the normal moveout of the deep reflecting horizons. The top part of this record is dominated by reflections from above-ground targets, such as cars, buildings, and utility lines. We were able to verify that the deep reflections, i.e. below 100 nsec or 4 meters, are from within the earth based on a velocity analysis using the data on the sections. The circled

region labeled "1" on this cross section is the area of highest reflection strength. This region correlates well with the known mine workings in this area.

Limitations of GPR

The cross sections for the Tombstone survey show reflections down to depths of approximately 18 meters. The rocks in this area, primarily limestone, have a very high resistivity, which is an ideal environment for the application of GPR. Unfortunately, soil and rock are generally much more conductive than this, leading to a greatly reduced depth of investigation. The plots in Figures 11-14 (Sternberg and Levitskaya, 2001) show the range of electrical properties and penetration depths that are typically encountered in nature. These plots are based on measurements of samples made in the LASI Lab by Dr. Levitskaya and are from some of the areas where we have run surveys. The "W" values listed on these plots are the weight percent water contained in the sample. The attenuation is lower and the depth of penetration is greater at lower frequencies, in all cases, which is why we designed the LASI ellipticity system to operate at lower frequencies than most GPR systems. The samples from Brookhaven are clean sands and have very low attenuation values, i.e. similar to the Tombstone rocks. The Avra Valley samples are representative of most soils and rocks in the southwestern U.S. and have too high an attenuation for effective GPR surveys at depths of interest for many abandoned underground mine problems, using antenna center frequencies of 100s of MHz.

A new approach to low-frequency imaging

The Federal Communications Commission has recently "discovered" ground penetrating radar. They have enacted new regulations that apply to GPR and other ultra-wideband transmissions in the radio frequency spectrum. All new GPRs must meet these requirements. Manufacturers of GPR equipment have found that they are able to use sufficient shielding and low enough transmitted power at frequencies above approximately 100-200 MHz to meet these requirements. The manufacturers have said that they do not see any way to meet these regulations for frequencies below 100 MHz. We have therefore been working on an alternative transmission strategy below 100 MHz. Table 1 lists frequencies known as Industrial, Scientific, and Medical (ISM) frequency bands. It is possible to transmit relatively large powers without a license in these frequency bands. These are narrow bands but are distributed well throughout the region between 1 and 50 MHz. With support from the National Science Foundation (Grant # 0097324), we are studying the applicability of a method known as Model Based Parameter Estimation (MBPE), Miller and Burke, 1991, to interpolate the data between the ISM frequencies. A key step in the application of the the MBPE technique to these data is preprocessing, as summarized in Figure 15. Figure 16 shows the results of using MBPE after pre-processing the data to interpolate wideband data from the narrow band measurements at the ISM frequencies (Matai et al., 2004). The curve labeled EM1DSH is a calculation from a layered-earth modeling code, which is applicable at all frequencies. The ISM measurements are shown by the X symbols. The MBPE predictions using the ISM data are shown by the dashed curves. One of the challenges in this procedure is to choose the correct model order for the MBPE algorithm. We have found that the model order that best fits the data at the ISM

frequencies also predicts the data best in between the ISM frequencies. This method looks promising and it does appear possible to synthesize a wideband response from narrowband measurements at the ISM frequencies.

References

Henley, Michael L., Ben K. Sternberg, 2000, Ground Penetrating Radar (GPR) surveys in Tombstone, Arizona, Final report to State Mine Inspector's Office and the City of Tombstone, February 15, 2000.

Matai, M., B.K. Sternberg, S.L. Dvorak, 2004, Synthesis of Wideband Earth Responses from Narrowband Measurements using Model Based Parameter Estimation, In preparation.

Miller, E.K., G.J. Burke, 1991, Using model- based parameter estimation to increase the physical interpretability and numerical efficiency of computational electromagnetics, Computer Physics Communications, 68, 43-75.

Poulton, M.M. and B.K. Sternberg, 1995, Identifying subsidence hazards using a unique high-resolution EM system and neural network interpretation, U.S. Bureau of Mines, Abandoned Mine Land Program, Contract #1432-J0220004.

Sternberg, B.K., Miletto, M.F., LaBrecque, D.J., Thomas, S.J., Poulton, M.M., 1991, revised Dec. 1992, The Avra Valley (Ajo Road) Geophysical Test Site: geophysical surveys, geologic data, and initial development of the test site, LASI-91-2, University of Arizona, Laboratory for Advanced Subsurface Imaging, Tucson, AZ.

Sternberg, B.K. and M.M. Poulton, 1995, Subsurface void detection using a unique high-resolution EM imaging system and neural network interpretation, U.S. Army Corps of Engineers, Waterways Experiment Station, Contract #DAAK 70-92-C-0065.

Sternberg, B.K. and M.M. Poulton, 1996, LASI ellipticity survey at the Nevada Test Site for Sandia National Laboratories, Final Report, Sandia Contract #AS-2042-0144.

Sternberg, B.K., 1999, A New Method of Subsurface Imaging – The LASI High Frequency Ellipticity System: Part 1. System Design and Development, JEEG, 4, 4, p. 197-213.

Sternberg, B.K., S.J. Thomas, R.A. Birken, 1999, A New Method of Subsurface Imaging – The LASI High Frequency Ellipticity System: Part 2. Data Processing and Interpretation, JEEG, 4, 4, p. 215-226.

Sternberg, B.K., R.A. Birken, 1999, A New Method of Subsurface Imaging – The LASI High Frequency Ellipticity System: Part 3. System Tests and Field Surveys, JEEG, 4, 4, p. 227-240.

Sternberg, B. K., X. Yang, 1999, Electromagnetic modeling using a thin-sheet approximation for non-sheet-like targets, JEEG, 4, 3, 167-178.

Sternberg, Ben K., Tsylya M. Levitskaya, 2001, Electrical parameters of soils in the frequency range from 1 kHz to 1 GHz, using lumped-circuit methods, Radio Science, 36, 4, 709-719, July/August.

Figure 1. Photograph of the transmitter all-terrain vehicle with the transmitting antenna suspended from the boom in the front of the ATV.

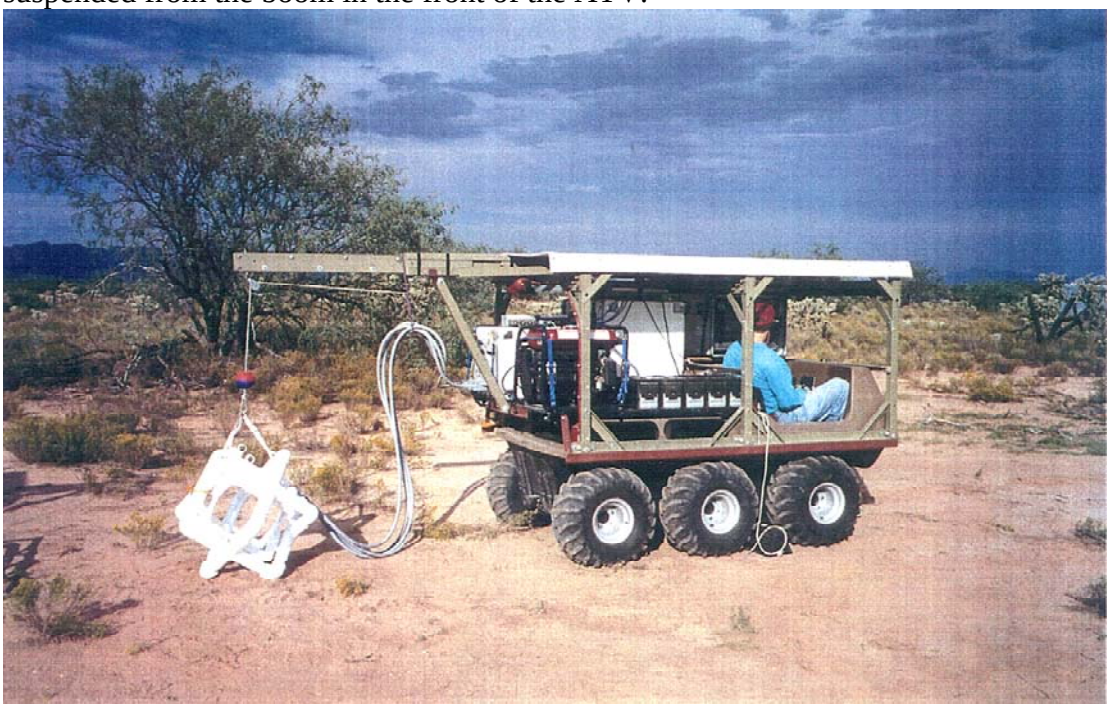

Figure 2. Photograph of the receiver all-terrain vehicle with the receiver antenna suspended from the boom projecting behind the ATV. In normal field operation this receiver ATV leads and the transmitter ATV follows along the profile line.

Figure 3. Photograph of the tunnel constructed at the University of Arizona, Avra Valley Geophysical Test Site.

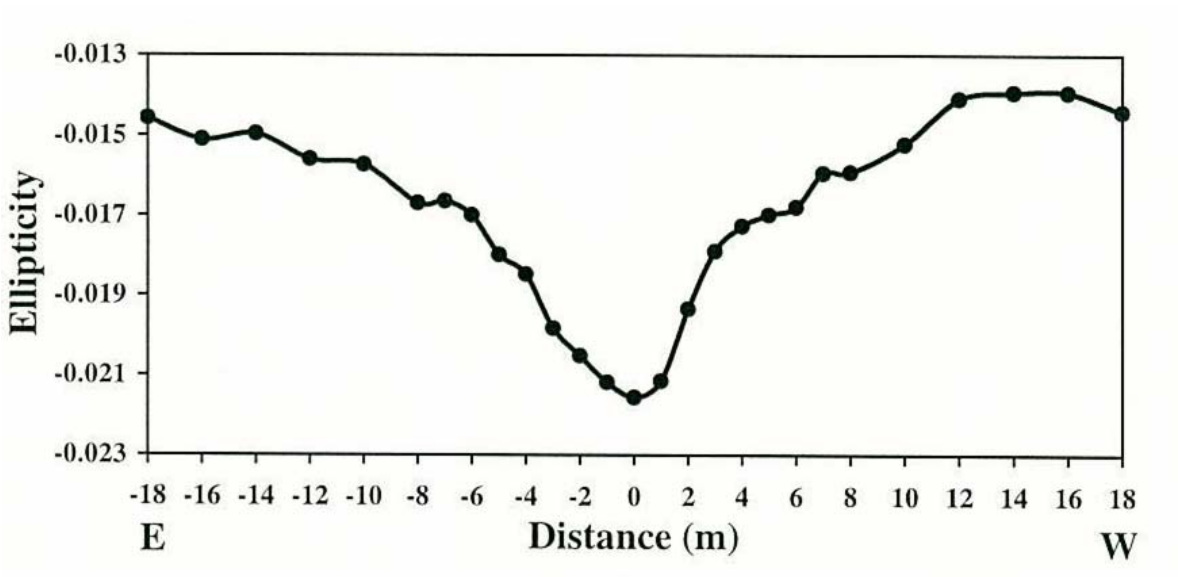

Figure 4. 8 meter broadside array over empty tunnel, 8 kHz.

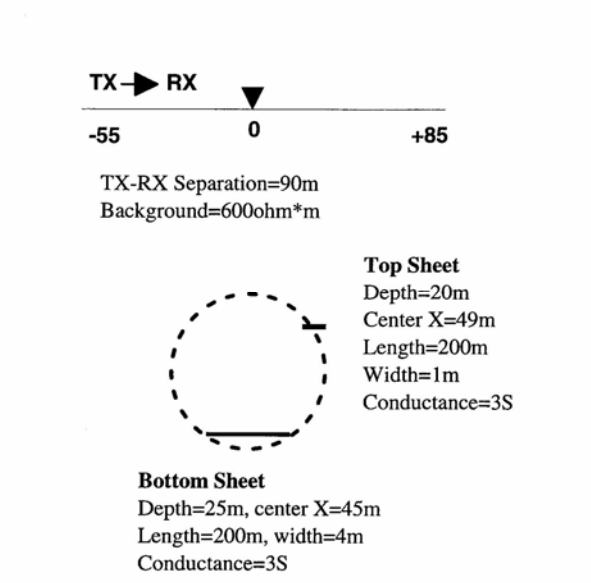

Figure 5. Model used for calculations of the EM response for the Nevada Test Site (NTS) Tunnel. Note, depth not to scale.

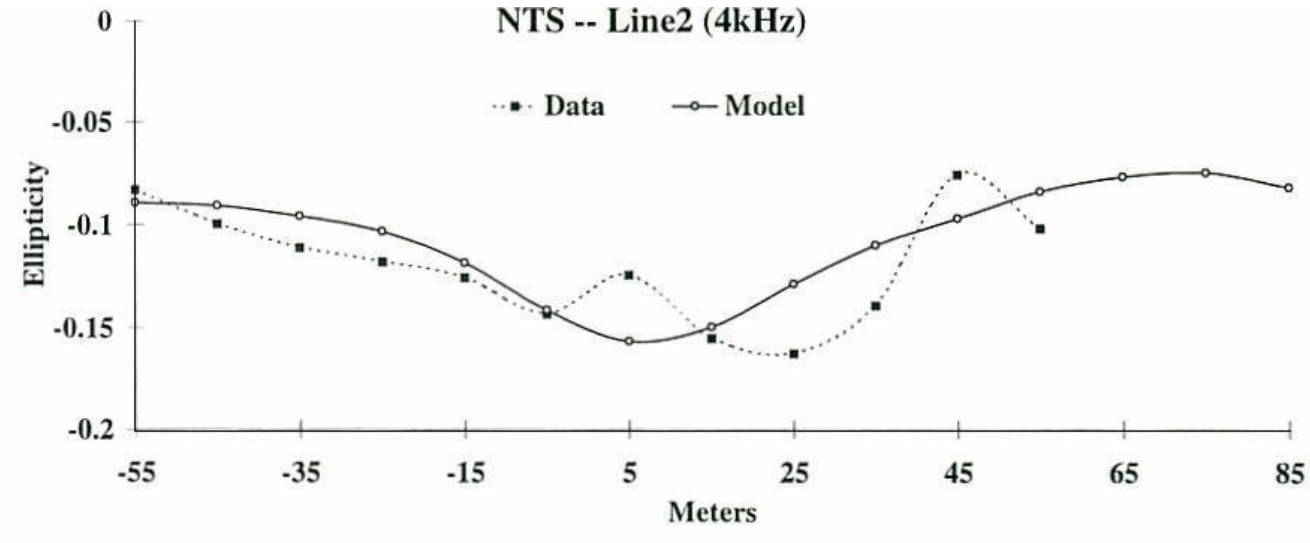

Figure 6. Comparison of data and theoretically calculated model ellipticities at the Nevada Test Site Tunnel.

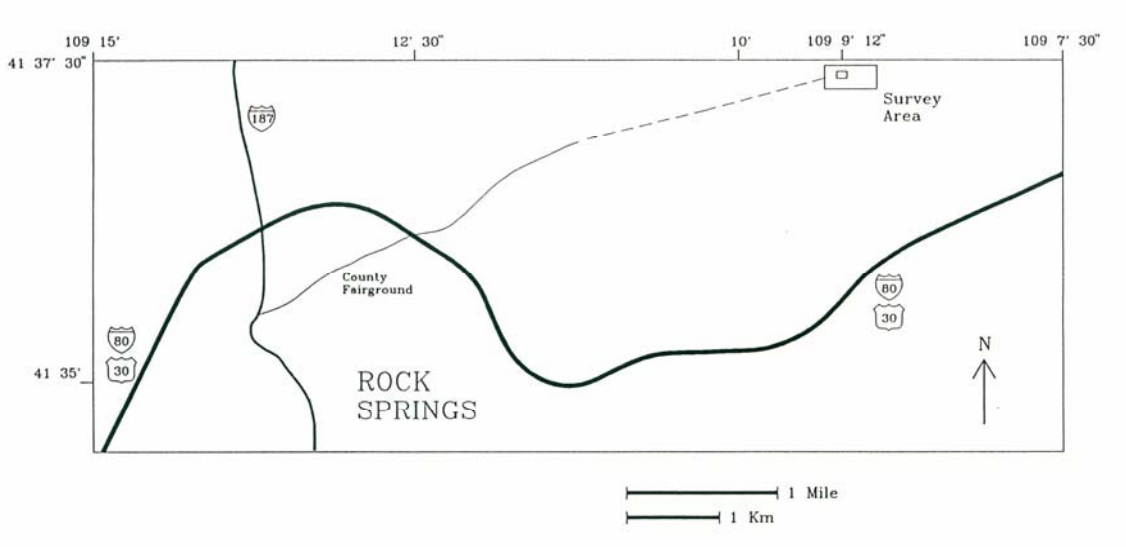

Figure 7. Location of the field survey near Rock Springs, Wyoming.

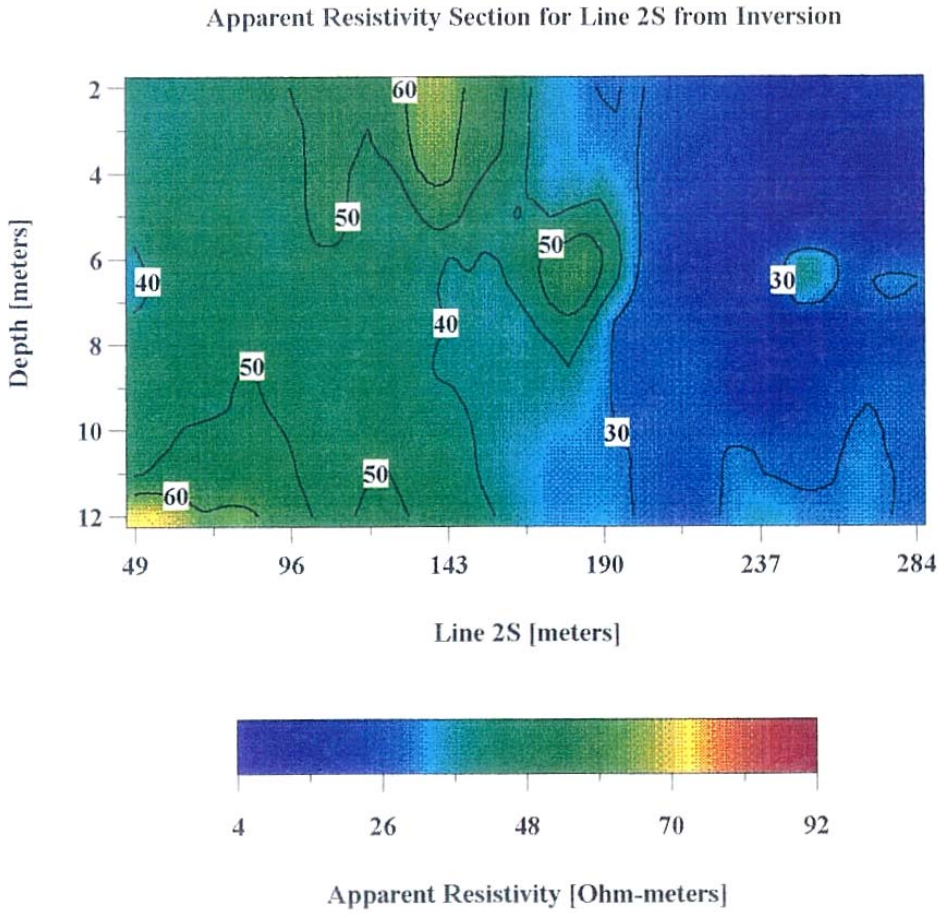

Figure 8. Resistivity section for line 2S created from apparent resistivity inversion results.

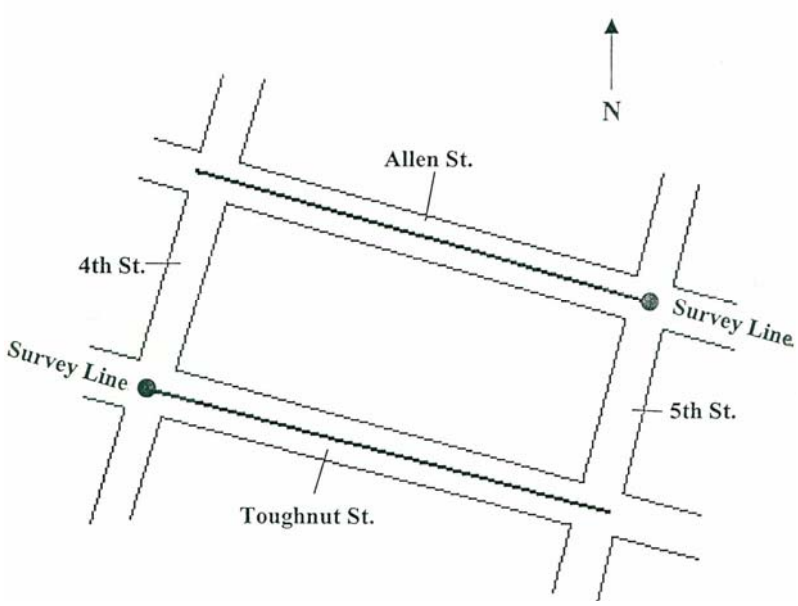

Figure 9. GPR survey locations at Tombstone, Arizona.

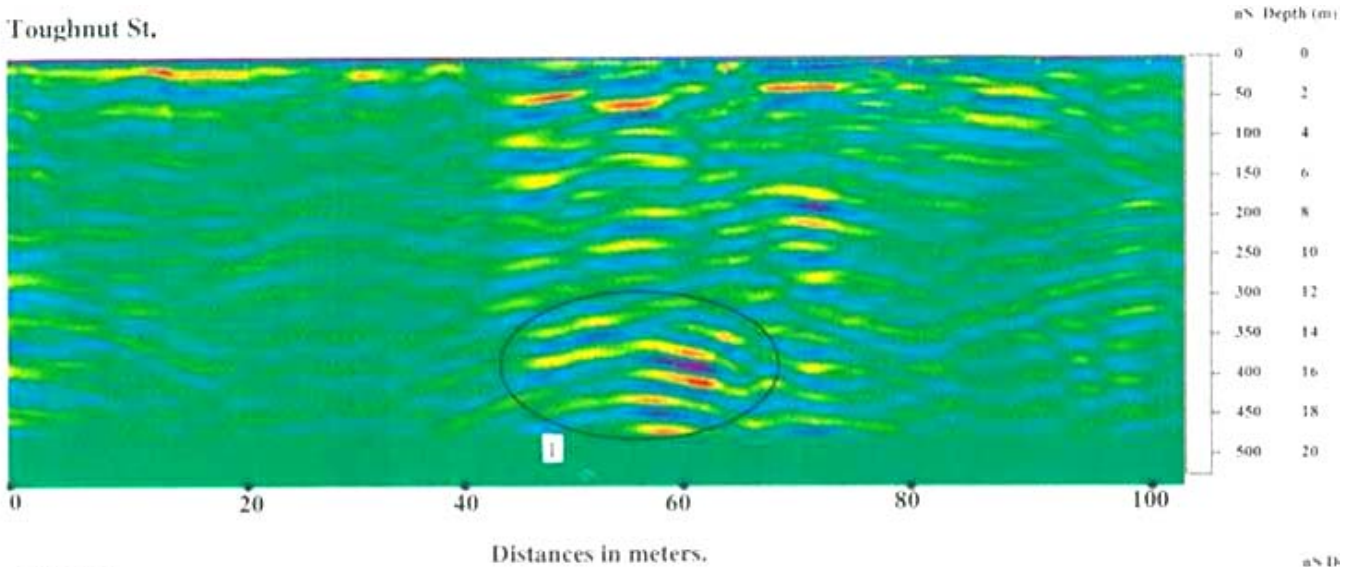

Figure 10. Toughnut St. GPR profile.

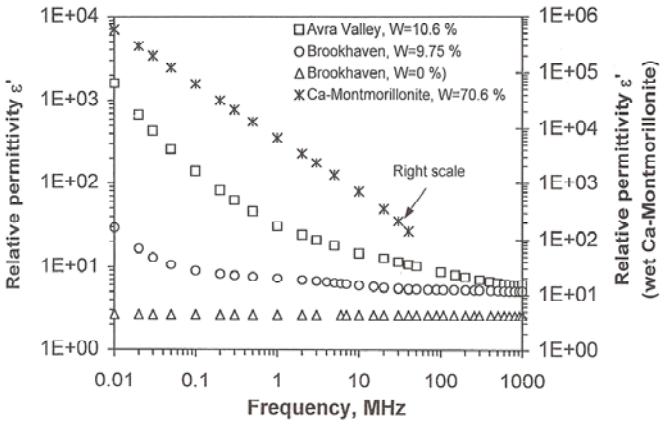

Figure 11. Relative permittivity.

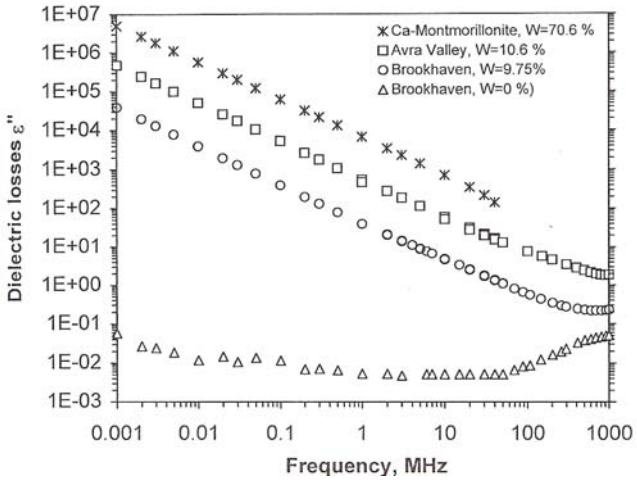

Figure 12. Dielectric losses.

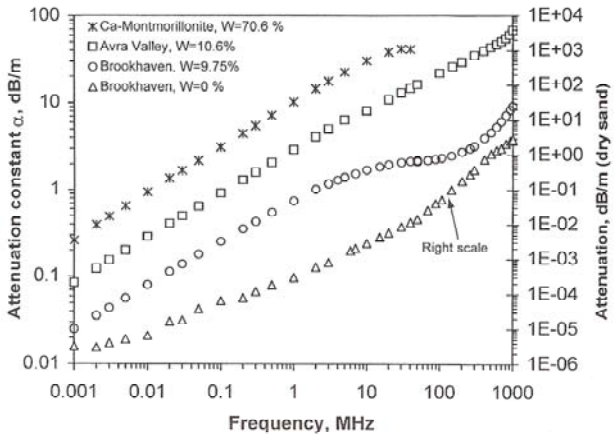

Figure 13. Attenuation constant.

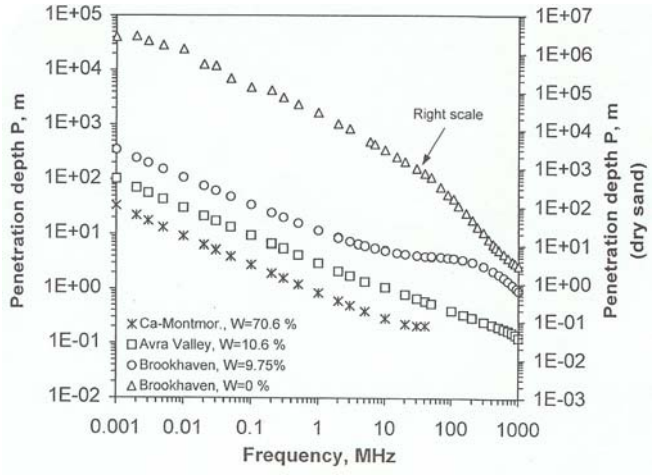

Figure 14. Penetration depth.

Center frequency (MHz)	Bandwidth (kHz)	Bandwidth (%)
6.78	+/- 15	0.44
13.56	+/- 7	0.10
27.12	+/- 163	1.20
40.68	+/- 20	0.10

Table 1 Characteristics of the ISM frequency bands.

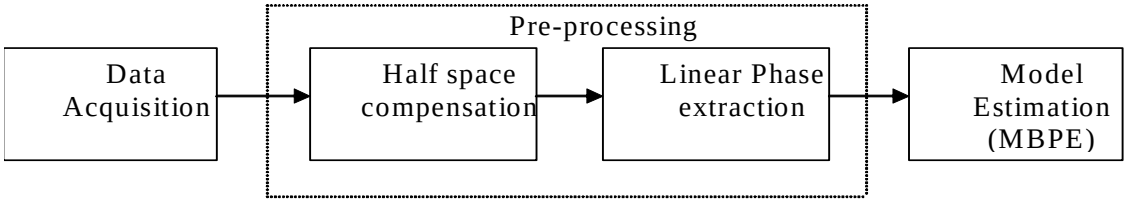

Figure 15. Block diagram of the modeling process.

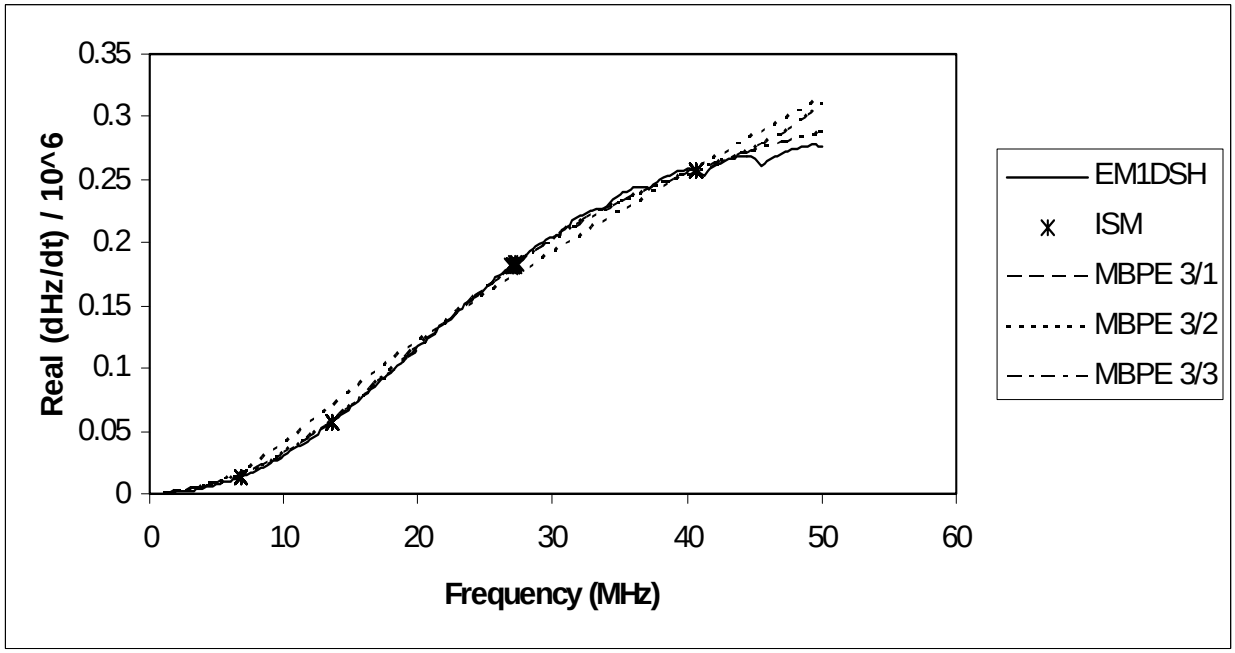

Figure 16. Data estimated for a three-layer model with thicknesses = 2m and 3m. Layer resistivities correspond to water contents of 5%, 10%, and 5%.